ISSN 1674-1056
http://cpb.iphy.ac.cn
http://iopscience.iop.org/cpb
中国物理 B
Chinese Physics
中国物理 Chinese Physics B

Design of scale model of plate-shaped absorber in wide frequency range

Li-Ming Yuan(袁黎明), Yong-Gang Xu(许勇刚), Wei Gao(高伟), Fei Dai(戴飞), Qi-Lin Wu(吴琪琳)
Citation: Chin. Phys. B . 2018, 27(4): 044101. **doi:** 10.1088/1674-1056/27/4/044101

Journal homepage: http://cpb.iphy.ac.cn; http://iopscience.iop.org/cpb

What follows is a list of articles you may be interested in

A broadband cross-polarization conversion anisotropic metasurface based on multiple plasmon resonances

M Ismail Khan, Farooq A Tahir
Chin. Phys. B . 2018, 27(1): 014101. **doi:** 10.1088/1674-1056/27/1/014101

Ultra-broadband and polarization-independent planar absorber based on multilayered graphene

Jiao Wang(王娇), Chao-Ning Gao(高超宁), Yan-Nan Jiang(姜彦南), Charles Nwakanma Akwuruoha
Chin. Phys. B . 2017, 26(11): 114102. **doi:** 10.1088/1674-1056/26/11/114102

An electrically tunable metasurface integrated with graphene for mid-infrared light modulation

Zongpeng Wang(王宗鹏), Ya Deng(邓娅), LianFeng Sun(孙连峰)
Chin. Phys. B . 2017, 26(11): 114101. **doi:** 10.1088/1674-1056/26/11/114101

Electromagnetic backscattering from one-dimensional drifting fractal sea surface II:Electromagnetic backscattering model

Tao Xie(谢涛), William Perrie, Shang-Zhuo Zhao(赵尚卓), He Fang(方贺), Wen-Jin Yu(于文金), Yi-Jun He(何宜军)
Chin. Phys. B . 2016, 25(7): 074102. **doi:** 10.1088/1674-1056/25/7/074102

Electromagnetic backscattering from one-dimensional drifting fractal sea surface I: Wave-current coupled model

Tao Xie(谢涛), Shang-Zhuo Zhao(赵尚卓), William Perrie, He Fang(方贺), Wen-Jin Yu(于文金), Yi-Jun He(何宜军)
Chin. Phys. B . 2016, 25(6): 064101. **doi:** 10.1088/1674-1056/25/6/064101

Design of scale model of plate-shaped absorber in a wide frequency range*

Li-Ming Yuan(袁黎明)[1,†], Yong-Gang Xu(许勇刚)[1], Wei Gao(高伟)[1], Fei Dai(戴飞)[1], and Qi-Lin Wu(吴琪琳)[2]

[1] *Science and Technology on Electromagnetic Scattering Laboratory, Shanghai* 200438, *China*
[2] *Key Laboratory of High Performance Fibers & Products, Ministry of Education, Donghua University, Shanghai* 201620, *China*

(Received 18 October 2017; revised manuscript received 7 December 2017; published online 10 March 2018)

In order to design the scale model in a wide frequency range, a method based on the reflective loss is proposed according to the high-frequency approximation algorithm, and an example of designing the scale model of a plate-shaped absorber is given in this paper. In the example, the frequency of the full-size measurement ranges from 2.0 GHz to 2.4 GHz, the thickness of the full-size absorber is 1 mm and the scale ratio is 1/5. A two-layer scale absorber is obtained by the proposed method. The thickness values of the bottom and top layer are 0.4 mm and 0.5 mm, respectively. Furthermore, the scattering properties of a plate model and an SLICY model are studied by FEKO to verify the effectiveness of the designed scale absorber. Compared with the corresponding values from the theoretical scale model, the average values of the absolute deviations in 10 GHz∼12 GHz are 0.53 dBm^2, 0.65 dBm^2, 0.76 dBm^2 for the plate model and 0.20 dBm^2, 0.95 dBm^2, 0.77 dBm^2 for the SLICY model while the incident angles are 0°, 30°, and 60°, respectively. These deviations fall within the Radar cross section (RCS) measurement tolerance. Thus, the work in this paper has important theoretical and practical significance.

Keywords: scale model, plate-shaped absorber, wide frequency range, RCS

PACS: 41.20.Jb, 81.70.Ex, 81.05.Qk **DOI:** 10.1088/1674-1056/27/4/044101

1. Introduction

The radar cross section (RCS) plays a very important role in object recognition, electronic warfare technology, etc. The most common methods to acquire the RCS of an object include the full-size measurement and the scale measurement.[1–4] As the full-size measurement is accompanied by many difficulties, such as falling short of the full-size object, poor controllability, expensive cost etc, the scale measurement has received increasing attention and it is widely applied to the study of the scattering properties. The classic scale theory was proposed by Stratton[5] and Sinclair[6] on the basis of the linear theory of Maxwell's equations. It is required that the scale system have the same electrical size as the full-size system, which means that the electromagnetic parameters of all materials in both systems are identical at the corresponding frequencies. Then, $\sigma_{\text{scale}} = \sigma_{\text{full}} + 20\lg p$, where σ_{scale} is the RCS of the scale model at the scale frequency, σ_{full} is the RCS of the full-size model at the full-size frequency, and p is the scale ratio.

In the scale measurement, it is crucial to construct an accurate scale model. Because there is little difficulty in constructing a satisfactory model for a perfect electric conductor (PEC) or weak loss dielectric materials, existing studies of the scale measurement mainly focus on the models composed of these materials.[7–11] However, many engineering materials, such as absorbers, have obvious frequency-dependent properties in the full-size frequency range.[12–14] Meanwhile, as the broadband radar can effectively improve the detection resolution to meet the requirement for the high-precision detection, the scattering properties of an object in a wide frequency range have attracted a great deal of attention. It is almost impossible to fabricate the scale material in the scale frequency range which has identical frequency-dependent properties with the theoretical scale material. Thus, it is urgent to develop some other principles to promote the development of the scale measurement in engineering.

In this paper, a method of designing the scale model in a wide frequency range based on the reflective loss is proposed according to the high-frequency approximation algorithm, and the design procedure is introduced in detail. An example is given to verify the effectiveness of the method, where a plate model and an SLICY model are constructed. Their scattering properties are simulated by FEKO and comparisons between the designed scale model and the theoretical scale model are performed.

2. Theories and methods

2.1. High-frequency approximation algorithm

According to the high-frequency approximation algorithm in electromagnetic scattering theories, the scattering electric field and magnetic field of a target can be determined

*Project supported by the National Natural Science Foundation of China (Grant Nos. 61601299 and 11404213), the Shanghai Municipal Science and Technology Commission, China (Grant Nos. 17210730900 and 15ZR1439600), and the Defense Industrial Technology, China (Grant No. B2120132001).

†Corresponding author. E-mail: lming_y@163.com

© 2018 Chinese Physical Society and IOP Publishing Ltd

by the induced electric current and magnetic current on its surface, and the scattering field of the target can be calculated by the Stratton–Chu formula,[15] which is expressed as follows:

$$\boldsymbol{E}^s = \frac{\mathrm{j}k}{4\pi}\frac{\mathrm{e}^{-\mathrm{j}kr}}{r}\int_s \hat{s}\times(\boldsymbol{M}_s + \eta_0\hat{s}\times\boldsymbol{J}_s)\,\mathrm{e}^{\mathrm{j}k\boldsymbol{r}'\cdot(\hat{s}-\hat{i})}\,\mathrm{d}s', \tag{1}$$

$$\boldsymbol{H}^s = -\frac{\mathrm{j}k}{4\pi}\frac{\mathrm{e}^{-\mathrm{j}kr}}{r}\int_s \hat{s}\times(\boldsymbol{J}_s - \frac{1}{\eta_0}\hat{s}\times\boldsymbol{M}_s)\,\mathrm{e}^{\mathrm{j}k\boldsymbol{r}'\cdot(\hat{s}-\hat{i})}\,\mathrm{d}s', \tag{2}$$

where $\boldsymbol{E}^s$ and $\boldsymbol{H}^s$ are the scattering electric field and magnetic field, respectively; $\boldsymbol{M}_s$ and $\boldsymbol{J}_s$ are the induced electric current and magnetic current on the surface of the target, respectively; η_0 is the impedance in free space; k is the propagation constant in free space; r is the distance from the observing location to the target; $\hat{s}$ and $\hat{i}$ are the unit vectors of the scattering direction and the incident direction, respectively; S is the entire surface of the target. The induced electric current and magnetic current are calculated by the following expressions:

$$\boldsymbol{J}_s = (\boldsymbol{H}^i + \boldsymbol{H}^r)\times\hat{n}, \tag{3}$$

$$\boldsymbol{M}_s = \hat{n}\times(\boldsymbol{E}^i + \boldsymbol{E}^r), \tag{4}$$

where $\boldsymbol{E}^i$ and $\boldsymbol{H}^i$ are the incident electric field and magnetic field, respectively; $\hat{n}$ is the unit normal vector of the surface. In Eqs. (3) and (4), $\boldsymbol{E}^r$ and $\boldsymbol{H}^r$ can be written as the following expressions,

$$\boldsymbol{E}^r = (\boldsymbol{E}^i\cdot\hat{v}^i_\perp)R_\perp\hat{v}^r_\perp + (\boldsymbol{E}^i\cdot\hat{v}^i_\parallel)R_\parallel\hat{v}^r_\parallel, \tag{5}$$

$$\boldsymbol{H}^r = (\boldsymbol{H}^i\cdot\hat{v}^i_\perp)R_\parallel\hat{v}^r_\perp + (\boldsymbol{H}^i\cdot\hat{v}^i_\parallel)R_\perp\hat{v}^r_\parallel, \tag{6}$$

where $\hat{v}$ denotes a unit vector; i and r represent the incidence and reflection, respectively; $\parallel$ and $\perp$ refer to the normal direction and tangential direction, respectively. The integral part $\int_s \mathrm{e}^{\mathrm{j}k\boldsymbol{K}\cdot\boldsymbol{r}'}\,\mathrm{d}s'$ in the scale system is almost the same as the full-size system. According to the above formulae, it can be deduced that the calculated results of the scattering electric field and magnetic field are identical as the reflection coefficients are the same everywhere on the surface of the target. Thus, the scale model of an electromagnetic absorber can be designed by the reflective loss (RL). This approach brings two important benefits: on the one hand, the electromagnetic parameters of the scale absorber can be different from those of the full-size absorber; on the other hand, the geometric sizes, such as the thickness, are free from the limitation of the scale ratio. These two points will make it easy to construct the scale absorber in engineering.

2.2. Calculating the RL of a multilayer absorber

It is known that a single layer absorber can always be optimized to have a specific RL at a single frequency or in a very narrow frequency range.[16] In order to make the absorber have the required RL in a wide frequency range, a multilayer absorber is a good candidate. Figure 1 shows the schematic description for calculating the reflection coefficient of an n-layer absorber irradiated obliquely by the plane microwave.

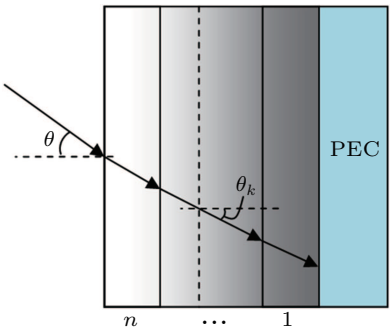


Fig. 1. (color online) Schematic description for calculating the reflection coefficient of an n-layer absorber irradiated obliquely by the plane microwave.

As the absorber is irradiated obliquely by the plane microwave, the RL is associated with the microwave polarization mode. TE wave and TM wave are the most common modes, and the RL of a multilayer absorber irradiated by TE wave and TM wave could be calculated from the following formulae,[17] respectively:

$$\mathrm{RL}_{TE} = 20\lg\left|\frac{Z_{\mathrm{in},n}\cos\theta - Z_0}{Z_{\mathrm{in},n}\cos\theta + Z_0}\right|, \tag{7a}$$

$$\mathrm{RL}_{TM} = 20\lg\left|\frac{Z_{\mathrm{in},n} - Z_0\cos\theta}{Z_{\mathrm{in},n} + Z_0\cos\theta}\right|, \tag{7b}$$

where the bottom layer and the top layer denote the 1st layer and the n-th layer, respectively; θ is the incident angle, Z_0 is the impedance with the value of 377 Ω in free space, and $Z_{\mathrm{in},n}$ is the input impedance of the top layer and can be derived from the following recursion formulae:

$$Z_{\mathrm{in},1} = Z_0 Z_1\tanh(\gamma_1 d_1), \tag{8}$$

$$Z_{\mathrm{in},k} = Z_k\frac{Z_{\mathrm{in},k-1} + Z_k\tanh(\gamma_k d_k)}{Z_k + Z_{\mathrm{in},k-1}\tanh(\gamma_k d_k)}, \quad (k = 2,\ldots,n), \tag{9}$$

where Z_k, γ_k, and d_k are the impedance, the propagation constant, and the thickness of the k-th layer, respectively. The γ_k can be calculated from the following equation:

$$\gamma_k = \mathrm{j}\frac{2\pi f}{C}\sqrt{\mu_k\varepsilon_k}\cos\theta_k, \tag{10}$$

where ε_k and μ_k are the permittivity and permeability of the k-th layer, respectively; f is the frequency, C is the microwave propagation velocity in free space, θ_k is the incident angle in the k-th layer and it can be calculated by the following equation:

$$\cos\theta_k = \sqrt{1 - \frac{\sin^2\theta}{\mu_k\varepsilon_k}}. \tag{11}$$

In Eq. (9), Z_k can be calculated from the following equation as the absorber is irradiated by TE wave:

$$Z_k^{\mathrm{TE}} = \frac{Z_0}{\cos\theta_k}\sqrt{\frac{\mu_k}{\varepsilon_k}}, \tag{12a}$$

while the absorber is irradiated by TM wave,

$$Z_k^{\mathrm{TM}} = Z_0 \cos\theta_k \sqrt{\frac{\mu_k}{\varepsilon_k}}. \tag{12b}$$

Combining Eq. (7)–Eq. (12), the RL of a multilayer absorber could be calculated. On the basis of the RL, the scale model of a plate-shaped absorber in a wide frequency range can be designed.

2.3. Optimizing the RL of the scale absorber in a wide frequency range

The RL of a multilayer absorber is determined by these factors including the number of layers, the thickness and the electromagnetic parameters of each layer. Optimizing these parameters is the core of designing the scale model of an absorber in a wide frequency range, which will make the RL of the designed scale absorber identical with that of the theoretical scale absorber as much as possible at any incident angle. The optimizing procedure includes the following four steps.

(i) Input data

The data include the RL matrix of the theoretical scale absorber, which is comprised of the RLs at a series of frequencies and incident angles, the maximum number of layers of the scale absorber, the maximum thickness of the scale absorber, the minimum thickness which meets the manufacturing requirements for engineering and the number of loop calculations.

(ii) Prepare electromagnetic parameters at scale frequencies

Select electromagnetic particles, such as carbonyl iron particles, ferrite particles, etc, prepare samples by mixing the selected particles with a binder in different proportions, and measure the electromagnetic parameters. Furthermore, fit the measured data by the effective medium theory and record the formula for calculating the electromagnetic parameters of each series composite which includes the same kind of electromagnetic particles.

Here, the famous G-BG formula[18,19] is used to fit the measured electromagnetic parameters. Since the G-BG formula is suitable for a composite including isotropic inclusions, nevertheless, anisotropic particles are always employed in engineering, such as disc-shaped particles, rod-shaped particles, etc, it is necessary to make some changes before using the G-BG formula. Here, the composite of the maximum inclusion concentration in each series is treated as a new matrix medium and the original matrix medium is treated as a new inclusion. From this perspective, the changed G-BG formula is written as follows:

$$p_{\mathrm{m}} \frac{\phi_{\mathrm{m}}^{1/t} - \phi_{\mathrm{e}}^{1/t}}{\phi_{\mathrm{m}}^{1/t} + A\phi_{\mathrm{e}}^{1/t}} + (1 - p_{\mathrm{m}}) \frac{\phi_{\mathrm{h}}^{1/s} - \phi_{\mathrm{e}}^{1/s}}{\phi_{\mathrm{h}}^{1/s} + A\phi_{\mathrm{e}}^{1/s}} = 0, \tag{13}$$

where t and s are percolation exponents, $A = (1 - p_{\mathrm{c}})/p_{\mathrm{c}}$ with p_{c} denoting the percolation threshold; p_{m} is the added volume fraction of the matrix medium to obtain the composite of low particle concentration, i.e., $p_{\mathrm{m}} = 1 - p_{\mathrm{l}}/p_{\mathrm{h}}$, with p_{h} and p_{l} being the particle volume fractions of the highest particle concentration composite and the lower particle concentration composite, respectively; ϕ_{e} is the parameter of the effective medium; ϕ_{m} and ϕ_{h} are the measured parameters of the matrix medium and the highest particle concentration composite, respectively. The values of t, s, and A can be obtained by fitting a group of the measured parameters. After ϕ_{m} and ϕ_{h} are measured and t, s, and A are determined, the electromagnetic parameters of any particle concentration composite can be calculated by Eq. (13).

(iii) Perform loop calculations at scale frequencies

In each loop calculation, generate parameters including the number of layers, the thickness, the particle kind and the particle concentration of each layer by normal distribution random functions. Record all the parameters. Calculate the electromagnetic parameters of each layer from the formulae obtained in step (ii). Calculate the RL matrix which is comprised of the RL at a series of frequencies and incident angles by combining Eqs. (7)–(12). Then calculate the deviation by comparing the calculated RL matrix with the RL matrix of the theoretical scale absorber and record the deviation.

Here, the deviation is defined as follows:

$$\sigma^k = \sqrt{\sum_{m=1}^{M} \sum_{n=1}^{N} \left(\mathrm{RL}_{m,n}^{k} - \mathrm{RL}_{m,n}^{\mathrm{full}}\right)^2}, \tag{14}$$

where M and N are the numbers of scale frequencies and incident angles, respectively; $\mathrm{RL}_{m,n}^{k}$ and $\mathrm{RL}_{m,n}^{\mathrm{full}}$ are the elements of the calculated RL matrix of the k-th calculation and the theoretical scale absorber.

(iv) Search the optimal result

After the loop calculations, find out the minimum deviation. Then the parameters of the optimal scale absorber, including the number of layers, the thickness, the particle kind and the particle concentration of each layer, could be obtained according to the records in the loop calculations.

3. Results and discussion

Here, an example is given to illustrate the procedure of designing the scale model of a plate-shaped absorber in a wide frequency range. Only the TE wave is taken into account because its design procedures are the same as those of the TM wave. The full-size frequency ranges from 2.0 GHz to 2.4 GHz, the scale ratio is 1/5. Then the scale frequency ranges from 10 GHz to 12 GHz. The thickness of the full-size absorber is 1 mm. The electromagnetic parameters of the theoretical scale absorber are the same as those of the

full-size absorber at corresponding frequencies in a range of 2.0 GHz–2.4 GHz, and the thickness of the theoretical scale absorber is 0.2 mm. According to the optimizing method introduced in Subsection 2.3, the designed scale absorber has two layers with a 0.4-mm-thick bottom layer and a 0.5-mm-thick top layer. The electromagnetic parameters of the theoretical scale absorber in a frequency range of 10 GHz–12 GHz are the same as those of the full-size absorber at the corresponding frequencies ranging from 2.0 GHz to 2.4 GHz. Figure 2 shows that the plots of frequency-dependent permittivity and permeability of the theoretical scale absorber and the two layers of the designed scale absorber in a frequency range of 10 GHz∼12 GHz.

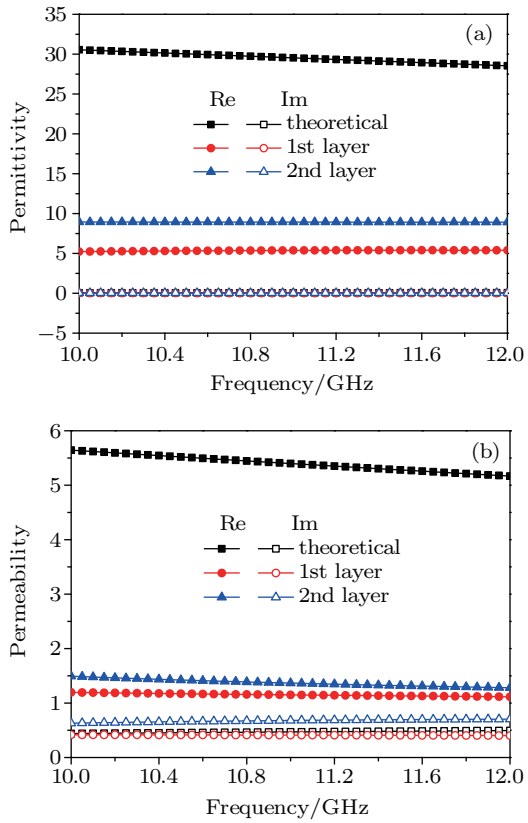


Fig. 2. (color online) Plots of frequency-dependent complex permittivity and permeability of the theoretical scale absorber and the designed scale absorber in a frequency range of 10 GHz–12 GHz.

Figure 3 shows the plots of the calculated incident-angle-dependent and frequency-dependent RL of the theoretical scale absorber and the designed scale absorber. As shown in Fig. 3(a), it is illustrated that the incident-angle-dependent RL changes as the incident angle at the selected scale frequencies of 10 GHz, 11 GHz, and 12 GHz, and it can be seen that the RLs between the theoretical scale absorber and the designed scale absorber are in good agreement at frequencies ranging from 0° to 85°. In Fig. 3(b) it is illustrated that the RL changes as the scale frequency at the selected incident angles of 0°, 30°, and 60°, and it can be seen that the RLs of the designed scale absorber accord well with those of the theoretical scale absorber in a frequency range of 10 GHz–12 GHz, where the average values of the absolute deviations are 0.012 dB, 0.0021 dB, and 0.0097 dB for 0°, 30°, and 60°, respectively.

In order to verify the effectiveness of the designed scale absorber, plate-shaped absorber models are constructed and the scattering properties are investigated by the commercial software FEKO. Here, the length of the full-size plate is 500 mm and its thickness is 1 mm. Thus, the theoretical scale plate has the length of 100 mm and the thickness of 0.2 mm. The designed scale plate has two layers with a 0.4-mm-thick bottom layer and a 0.5-mm-thick top layer, and both layers have a length of 100 mm.

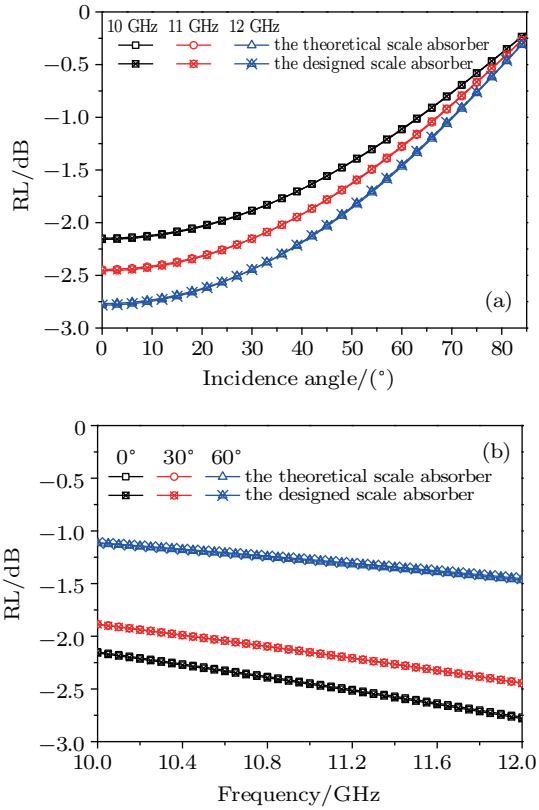


Fig. 3. (color online) RLs of theoretical scale absorber and designed scale absorber, showing their changes (a) as incident angle when scale frequencies are 10 GHz, 11 GHz, and 12 GHz, respectively, and (b) as the scale frequency when the incident angles are 0°, 30°, and 60°, respectively.

Figure 4 shows the simulated model of an absorber plate for studying the bi-static RCS and the simulated results of the theoretical scale plate and the designed scale plate at 10 GHz, 11 GHz, and 12 GHz. The plate is irradiated by TE wave in the normal direction. The observation point is located in the directions of the elevation angle ranging from 0° to 85° and the azimuth angle equal to 0°. As shown in Fig. 4(b), it can be seen that the bi-static RCS of the theoretical scale plate and that of the designed scale plate are in excellent agreement with each other, which means that the scattering property of the designed scale plate is very close to that of the theoretical scale plate.

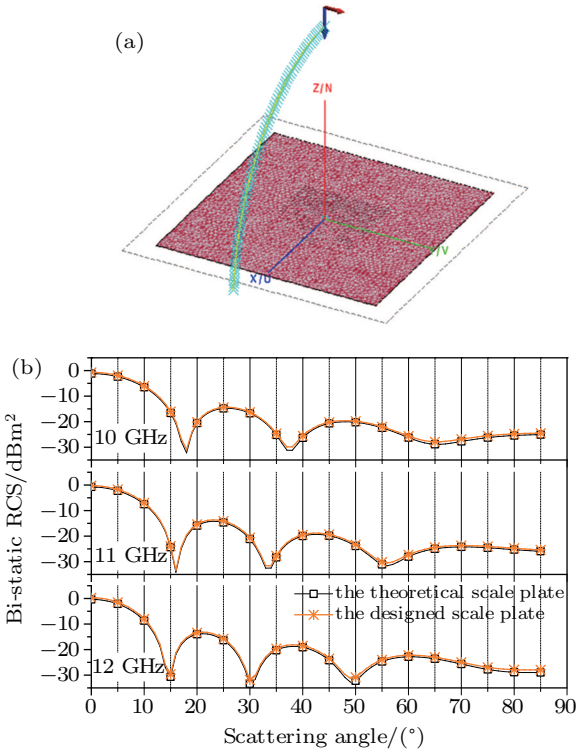


Fig. 4. (color online) (a) Simulation model of an absorber plate and (b) simulation bi-static RCS of the theoretical scale plate and the designed scale plate.

Meanwhile, the mono-static RCS of the theoretical scale plate and the designed scale plate are studied as the TE wave irradiates in the directions of the elevation angle ranging from 0° to 85° and the azimuth angle equal to 0°. Figure 5 shows the plots of the simulation results. As shown in Fig. 5(a), the mono-static RCS changes as the incident angle at the selected scale frequencies of 10 GHz, 11 GHz, and 12 GHz, and it can be seen that the results from the theoretical scale plate and the designed scale plate are in good agreement with each other. As shown in Fig. 5(b), the mono-static RCS changes as the scale frequency at the selected incident angles of 0°, 30°, and 60°, and it can be seen that the mono-static RCSs of the designed scale plate and the theoretical scale plate have the same change tendency in a frequency range of 10 GHz–12 GHz at the three incident angles. The closer to the normal direction of the plate the incident direction is, the better the mono-static RCS of the designed plate fits that of the theoretical scale plate. In 10 Hz–12 GHz, the average values of the absolute deviations are 0.53 dBm^2, 0.65 dBm^2, and 0.76 dBm^2 while the incident angles are 0°, 30°, and 60°, respectively. It is explained by the following two reasons: 1) the RL depends on the scattering properties in the reflecting direction and the mono-static RCS depends on the scattering properties in the anti-incidence direction. This means that the scattering properties in the anti-incidence direction can be different though the scattering properties in the reflecting direction are identical; 2) as shown in Fig. 3(b), the larger the incident angle is, the larger the deviations of the RL are.

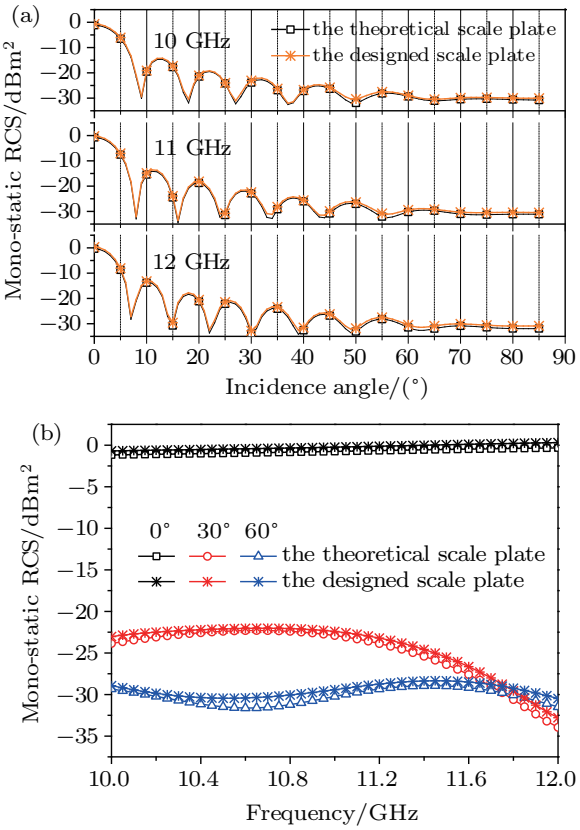


Fig. 5. (color online) The simulation mono-static RCSs of the theoretical scale plate and the designed scale plate, showing changes (a) with incident angle when the scale frequencies are 10 GHz, 11 GHz, and 12 GHz, respectively; (b) with scale frequency when the incident angles are 0°, 30°, and 60°, respectively.

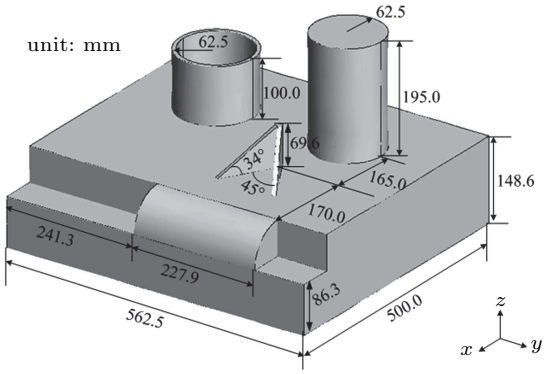


Fig. 6. Schematic description of the full-size SLICY model.

Furthermore, a complicated model, SLICY, which includes many electromagnetic scattering mechanisms such as specular-reflection, multiple-reflection, creeping wave scattering, cavity scattering, etc, is constructed and the mono-static RCS is simulated. Figure 6 illustrates the full-size SLICY model as well as its key geometric parameters. All the surfaces are coated by the full-size absorber. The TE wave irradiates the SLICY in the directions of the elevation angle ranging from 0° to 90° and the azimuth angle is equal to 0°.

The simulated results are plotted in Fig. 7. As shown in Fig. 7(a), the mono-static RCS changes as the incident an-

gle at the selected scale frequencies of 10 GHz, 11 GHz, and 12 GHz, and it can be seen that the results from the theoretical scale SLICY and the designed scale SLICY are in good agreement with each other. As shown in Fig. 7(b), the mono-static RCS changes as the scale frequency at the selected incident angles of 0°, 30°, and 60°, and it can be seen that the mono-static RCS of the designed scale SLICY and the theoretical scale SLICY have a similar change tendency in 10 GHz∼12 GHz at the three incident angles. The larger the incident angle is, the larger the deviation is. The average values of absolute deviations are 0.20 dBm^2, 0.95 dBm^2, and 0.77 dBm^2 while the incident angles are 0°, 30°, and 60°, respectively. The deviations are thought to come from the contribution of non-plane scattering sources to the SLICY. However, these deviations are still thought to be within the RCS measurement tolerance.

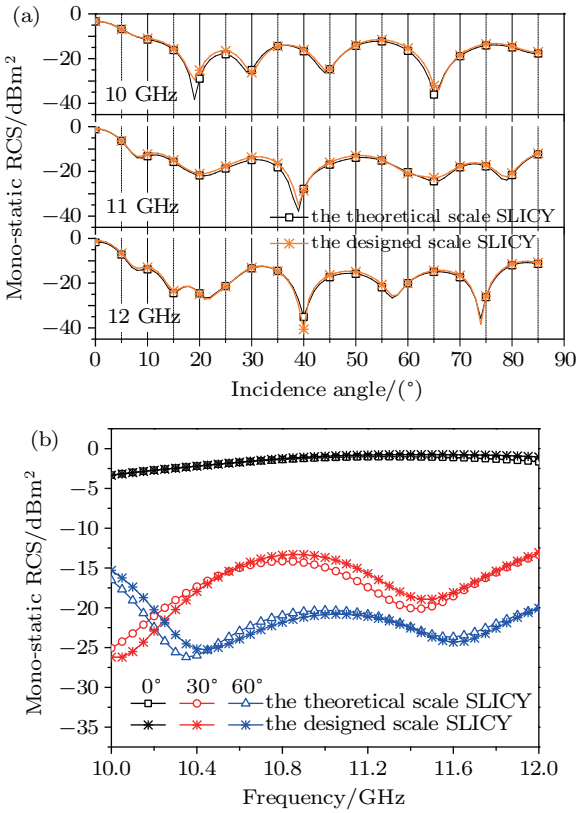


Fig. 7. (color online) Simulation mono-static RCSs of the theoretical scale SLICY and the designed scale Slicy, showing changes (a) with incident angle when scale frequencies are 10 GHz, 11 GHz, and 12 GHz, respectively, and (b) with scale frequency when the incident angles are 0°, 30°, and 60°, respectively.

4. Conclusions

According to the high-frequency approximation algorithm, an effective method to design the scale model in a wide frequency range is proposed on the basis of the RL. By optimizing the parameters including the number of layers, the thickness, the particle kind and the particle concentration of each layer, the RL of the scale absorber is designed to be identical with the RL of the theoretical scale absorber as much as possible. An example of designing the scale model of a plate-shaped absorber in a wide frequency range is given to verify the effectiveness of the method. In the example, a plate model and a SLICY model are constructed and their scattering properties are simulated by FEKO. The average values of the absolute deviations in 10 GHz∼12 GHz are 0.53 dBm^2, 0.65 dBm^2, 0.76 dBm^2 for the plate model and 0.20 dBm^2, 0.95 dBm^2, 0.77 dBm^2 for the SLICY model while the incident angles are 0°, 30°, and 60°, respectively. These average values are comparable to the results from the theoretical scale model. These deviations fall within the RCS measurement tolerance. Thus, the work in this paper has important theoretical and practical significance.

It is worth pointing out that the scale ratio is small in the study. While the scale ratio is large, the scale frequency is always located in the millimeter/submillimeter wave band where regular materials have a weak loss property. Further research on the large scale ratio is still under way.

References

[1] Bird D 1994 *Radar Conference,* 1994*, Record of the* 1994 *IEEE National*, March 29–31, 1994, Atlanta, GA, USA, p. 74
[2] White M O 1998 *Electron. & Commun. Engin. J.* **10** 169
[3] Zhao Y, Zhang M and Chen H 2012 *IEEE Trans. Anten. Propag.* **60** 5890
[4] Hu C F, Zhou Z, Li N J and Zhang K 2014 *J. Syst. Engin. Electron.* **25** 588
[5] Stratton J 1941 *Electromagnetic Theory* (New York: McGrow-Hill)
[6] Sinclair G 1948 *Proc. Inst. Radio Eng.* **36** 1364
[7] De Adana F S, Gonzalez I, Gutierrez O and Catedra M F 2003 *IEE Proceedings-Radar, Sonar and Navigation* **150** 375
[8] Susetio A, Oki T and Morishita H 2015 *Antennas and Propagation (APCAP),* 2015 *IEEE 4th Asia-Pacific Conference*, June 30–July 3, 2015, Kuta, Indonesia, p. 568
[9] Jacobs B and Baker D 2012 *IEEE-APS Topical Conference on Antennas and Propagation in Wireless Communications (APWC)*, September 2–7, 2012, Cape Town, South Africa, p. 1001
[10] Gorji A B, Janalizadeh R C and Zakeri B 2013 *Proceedings of* 2013 *URSI International Symposium on Electromagnetic Theory (EMTS)*, May 20–24, 2013, Hiroshima, Japan, p. 1066
[11] Wang X B, He X Y, Wu Y J, Dai F and Li L 2013 *Green Computing and Communications (GreenCom),* 2013 *IEEE and Internet of Things (iThings/CPSCom), IEEE International Conference on and IEEE Cyber, Physical and Social Computing*, August 20–23, 2013, Beijing, China, p. 1587
[12] Liu T, Zhou P H, Liang D F and Deng L J 2012 *Chin. Phys. B* **21** 50302
[13] Mano J F 1998 *J. Phys. D: Appl. Phys.* **31** 2898
[14] Lagarkov A N and Rozanov K N 2009 *J. Magn. Magn. Mater.* **321** 2082
[15] Lee J S, Song T L, Du J K and Yook J G 2013 *IEEE Antennas and Propagation Society International Symposium (APSURSI)* 2013, July 7–13, 2013, Orlando, FL, USA, p. 606
[16] Yuan L M, Wang B, Gao W, Xu Y G, Wang X B and Wu Q L 2017 *Results in Physics* **7** 1698
[17] Kim J W and Kim S S 2010 *Materials & Design* **31** 1547
[18] McLachlan D S 1986 *J. Phys. C: Solid State Phys.* **19** 1339
[19] Chen P, Wu R X, Zhao T, Yang F and Xiao J Q 2005 *J. Phys. D: Appl. Phys.* **38** 2302